forests

MDPI

Article

Simulation and Prediction of the Potential Geographical Distribution of *Acer cordatum* Pax in Different Climate Scenarios

Mi-Li Liu [1,†], Hong-Yuan Sun [1,†], Xin Jiang [1], Tong Zhou [1], Qi-Jing Zhang [1], Zi-Dong Su [1], Ya-Ni Zhang [1], Jian-Ni Liu [2,*] and Zhong-Hu Li [1,*]

[1] Key Laboratory of Resource Biology and Biotechnology in Western China, Ministry of Education, College of Life Sciences, Northwest University, Xi'an 710069, China
[2] Early Life Institute, State Key Laboratory of Continental Dynamics, Department of Geology, Northwest University, Xi'an 710069, China
* Correspondence: elilJn@nwu.edu.cn (J.-N.L.); lizhonghu@nwu.edu.cn (Z.-H.L.); Tel./Fax: +86-29-88302411 (Z.-H.L.)
† These authors contributed equally to this work.

Abstract: By analyzing the effects of environmental variables on plants, changes in plant distribution as a result of climate oscillations can be studied, which is of great significance to plant protection and management policies. *Acer cordatum* Pax (Aceraceae) is a non-deciduous tree distributed in valleys and streams in eastern China. Due to the effects of changing climate (warmer, drier conditions) and human impacts, the number of wild individuals of *A. cordatum* has exhibited a decrease trend, which is in urgent need of protection. In this study, the maximum entropy algorithm (MaxEnt) was used to predict the potential geographical distribution of *A. cordatum* during the Last Interglacial (LIG), and Last Glacial Maximum (LGM), current, 2060s, and 2080s periods. The model used geographic location information of 337 *A. cordatum* and six climatic variables. The area under the receiver operating characteristic curves (AUC) of the simulation results were more than 0.95, indicating high accuracy in the simulation result. The mean temperature of coldest quarter, precipitation of warmest quarter, precipitation of driest month, and precipitation of seasonality were important climatic variables influencing the geographic distribution of *A. cordatum*. Based on the simulate results, the potential distribution areas of *A. cordatum* experienced a process of expansion and then contraction from LIG to the future. In the future, some potential suitable areas provinces will likely shrink (Guizhou, Fujian, and Anhui), even almost disappear (Chongqing), and the general distribution will trend to transfer in a northeastward direction. It is hoped that this study can provide a theoretical reference for the future protection of *A. cordatum*.

Keywords: climate change; species distribution modeling; potential suitable habitat; MaxEnt

Citation: Liu, M.-L.; Sun, H.-Y.; Jiang, X.; Zhou, T.; Zhang, Q.-J.; Su, Z.-D.; Zhang, Y.-N.; Liu, J.-N.; Li, Z.-H. Simulation and Prediction of the Potential Geographical Distribution of *Acer cordatum* Pax in Different Climate Scenarios. *Forests* **2022**, *13*, 1380. https://doi.org/10.3390/f13091380

Received: 28 July 2022
Accepted: 24 August 2022
Published: 29 August 2022

1. Introduction

There is a close relationship between environmental variables (i.e., solar, water, soil) and a plant species geographical distribution. Generally, plant distribution is significantly affected by long-term changes in climate [1]. As the planet warms, species distribution has also experienced significant changes across all major ecosystems on the Earth [2]. Studies show that many species face the risk of extinction under future climate change scenarios [3]. Large-scale climate changes have significantly affected the survival of endangered plant and animal species by reducing suitable habitats that facilitate plant community establishment and growth. Because of the smaller distribution area of these endangered plant species, plant observation, conservation, and research become more difficult. Therefore, the analyses of the impact of climate change for plant distribution are of great significance for species studies, which will provide a scientific basis for their management and protection.

Species distribution models (SDM) are used for the prediction of species distribution based on the realized niche of the species [4,5], and have been widely used in many

other fields, including global change ecology, population evolution, and environmental protection [6–8]. Currently, common SDM mainly include maximum entropy (MaxEnt) and random forest (RF) [9]. RF models consist of a series of decisional trees and randomly generated values that are used to build virtual forests [10]. MaxEnt is used to predict the best distribution area of a species by fitting its probability distribution of appearing in the target area and maximizing the entropy value of the probability distribution. MaxEnt provides greater accuracy in the prediction of the influence complex environmental variables will have on species that are distributed over a large area [11], and the results can be easily interpreted [12]. Fitzgerald et al. [13] used the MaxEnt method for predicting the niche changes of Bicknell's thrush (*Catharus bicknelli* Ridgeway) and the gray-cheeked thrush (*Catharus minimus* Lafresnaye) and they found balsam fir to be a major contributor to the distribution of Bicknell's thrush, whereas black spruce was found to be a major contributor to gray-cheeked thrush distribution.

Acer cordatum Pax belongs to the genus *Acer* of Aceraceae. It is a non-deciduous tree that is generally 7–10 m tall, with smooth bark that is mainly black and gray, and smooth twigs [14,15]. According to currently recorded specimens and related literature, *A. cordatum* is mainly distributed in the central and eastern coastal areas of China. *A. cordatum* is widely distributed in this region, and its distribution may also be highly influenced by a complex climate. It is common in mountains, forests, and valleys, generally distributed at an altitude of 500–1200 m. It has excellent foliage and fruit, making it a popular garden species [16]. In addition, *A. cordatum* have excellent resistance to heat, disease, and insects [17]. As a member of the *Acer*, *A. cordatum* can also be a donor of the leaf proteins [18].

Currently, the research on *A. cordatum* is limited [14,18], and few studies have focused on the effects of the environment on species. This study uses MaxEnt modeling to predict the relationship between the distribution area of *A. cordatum* and the historical and future climate environments. The purpose of this study is to determine the main climatic factors affecting the geographic distribution ranges of *A. cordatum*, and predict the changes of potential distribution of *A. cordatum* in the past and future periods. It is expected that this study will contribute to the identification of the suitable distribution area for *A. cordatum* in the future, and provide theoretical reference for the protection and research of *A. cordatum*.

2. Materials and Methods

2.1. Geographical Location Information Collection

The geographical distribution data (longitude and latitude) of *A. cordatum* was obtained from field investigation and online herbaria databases, including the Chinese Virtual Herbarium database (CVH, https://www.cvh.ac.cn/, accessed on 6 November 2021) and the Global Biodiversity Information Facility (GBIF, http://www.gbif.org/, accessed on 6 November 2021). In order to obtain highly accurate results, Boitani's [19] experience was referred to and the data was assessed. Some duplicated, and inaccurate of distribution points were removed in subsequent analyses. Ultimately, 337 reliable distribution points were used to perform the MaxEnt model program, of which 297 information points were from the CVH and 40 points were from the GBIF (Figure 1).

2.2. Climatic Variables Screening

The climate variables were obtained from the Global Climate Database (https://www.worldclim.org/, accessed on 6 November 2021) [20] in this research (Table 1). The spatial resolution was 2.5 arc minutes.

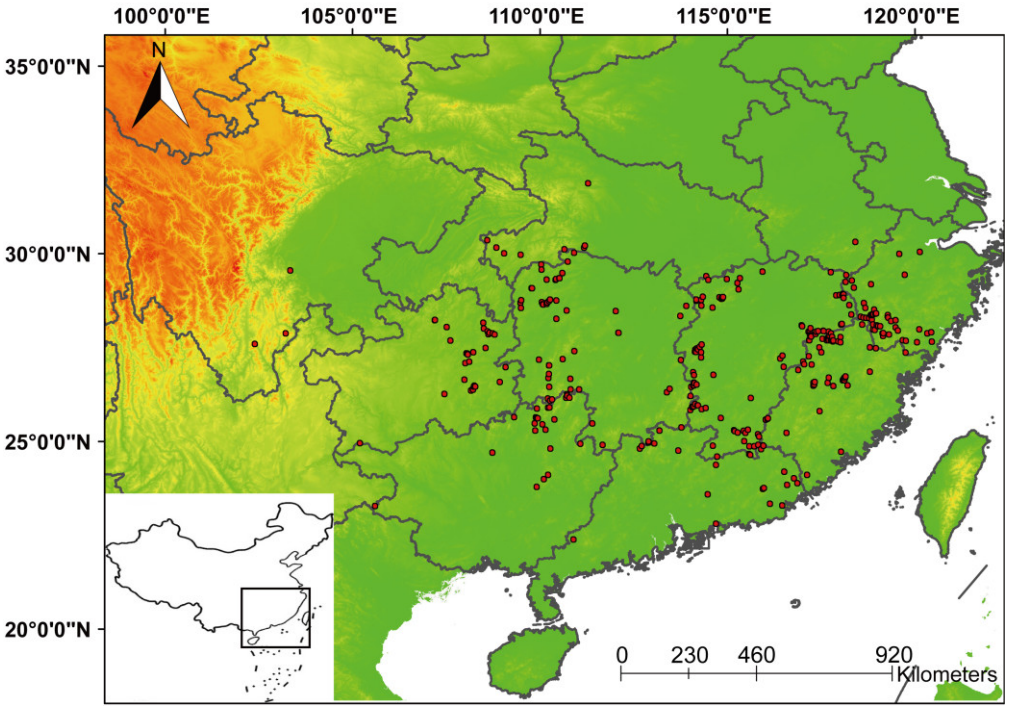

Figure 1. Geographic locations of distribution sites of *Acer cordatum* Pax in China. The map was quoted from the National Catalogue Service for Geographic Information (www.webmap.cn, accessed on 6 November 2021).

Table 1. The contribution of 19 climatic variables to the distribution of *Acer cordatum* Pax and explanations of each climatic variable.

Variable	Explanation	Percent Contribution
Bio14	Precipitation of Driest Month (mm)	67.9
Bio4	Temperature Seasonality (°C)	10.1
Bio18	Precipitation of Warmest Quarter (mm)	5.7
Bio12	Annual Precipitation (mm)	4.6
Bio8	Mean Temperature of Wettest Quarter (°C)	2.8
Bio11	Mean Temperature of Coldest Quarter (°C)	2
Bio3	Isothermality (bio2/bio7) (×100) (%)	1.9
Bio10	Mean Temperature of Warmest Quarter (°C)	1.9
Bio6	Min Temperature of Coldest Month (°C)	1
Bio9	Mean Temperature of Driest Quarter (°C)	0.6
Bio15	Precipitation of Seasonality (mm)	0.5
Bio2	Mean Diurnal Range (°C)	0.4
Bio7	Temperature Annual Range (°C)	0.3
Bio16	Precipitation of Wettest Quarter (mm)	0.1
Bio17	Precipitation of Driest Quarter (mm)	0.1
Bio19	Precipitation of Coldest Quarter (mm)	0.1
Bio1	Annual Mean Temperature (°C)	0
Bio5	Max Temperature of Warmest Month (°C)	0
Bio13	Precipitation of Wettest Month (mm)	0

To avoid the over-fitting of simulation results due to the mutual influence between the highly correlated climatic variables [21,22], the Pearson correlation coefficients analysis was performed between 19 climatic variables. Based on geographical distribution data of *A. cordatum* and 19 climatic factors, a MaxEnt model was initially established to evaluate the contribution of different variables to the distribution of climate data. A pair of climatic variables with correlation coefficients greater than $|0.85|$ were regarded as not independent

of each other. Finally, for each pair of significantly correlated variables, only one variable with a large contribution was used in the projection.

The potential distribution areas of *A. cordatum* were simulated for the five periods, including the Last Glacial Maximum (LGM), Last Interglacial (LIG), current (1970–2000 and released in January 2020), the 2060 years (2041–2060 years), and the 2080 years (2081–2100 years). Among them current, 2060s and 2080s are all from WorldClim version 2.1 (Global Climate Database: https://www.worldclim.org/, accessed on 6 November 2021). When simulating LGM, two variable factor models were used: Model for Interdisciplinary Research on Climate Earth System Model (MIROC) and Community Climate System Model (CCSM). MIROC is the result of simulation and prediction of the East Asian climate, and CCSM is the result of simulation and prediction of the global climate [23]. The distribution of *A. cordatum* is mainly concentrated within East Asia, so it was determined that the results of the MIROC simulation would provide greater accuracy. In the Future climatic factors, the Scenario Model Intercomparison Project (ScenarioMIP) is a new climate change scenario proposed by the sixth phase of the Coupled Model Intercomparison Project (CMIP6), which combines different shared socio-economic pathways with recent trends in anthropogenic emissions (SSP-RCP). In this study, the BCC-CSM2-MR data were selected from the lowest and highest trends (SSP1-2.6 and SSP5-8.5) for 2060s and 2080s as representatives to simulate the potential distribution areas of *A. cordatum* in the future (2060s and 2080s). Among them, SSP1-2.6 and SSP5-8.5 represent a green development pathway and the high end of the range of future pathways, respectively. The former will produce a multi-model mean of significantly less than 1.5 °C warming by 2100, while the latter will have a radiative forcing of 8.5 W/m^2 in 2100 [24].

2.3. Model Construction and Evaluation

The maximum entropy theory that was proposed by E.T. Jaynes [25] states that there are many ways of distributing random variables in restricted conditions, and choosing that with the largest entropy value as the distribution of the variable will have greater accuracy. Based on this principle, the selected map information is divided into mesh units by MaxEnt, and it maps the input geographic location and climate change factors to the mesh map units, achieving this through a comparison of the background geographic location information and the sample geographic location information prediction of species distribution. The maximum entropy model is based on probability theory and machine learning and uses the geographic location information of species and environmental change factors to construct the model. Relative Occurrence Rate (ROR) has an important correspondence with the output of MaxEnt. It determines the probability of a species appearing in other geographical locations based on the observed species sample. MaxEnt is an optimized algorithm that is used for the prediction of the probability of existence through Logistic Output (ROR transformation) [26]. This can be described as:

When the known x output is y for a given training data set and feature function, $f_i(x, y), i = 1, 2 \ldots, n$, MaxEnt solves the equation as:

$$\begin{aligned} &\max_{p \in c} H(P) - \sum_{x,y} \widetilde{P}(x) P(y|x) \log P(y|x) \\ &s.t. \quad E_p(f_i) = E_{\widetilde{P}}(f_i), i = 1, 2, \ldots, n \\ &\sum_{y} P(y|x) = 1 \end{aligned}$$

where: $H(P)$ is the conditional entropy, $P(y|x)$ is the conditional probability distribution hypothesis, $\widetilde{P}(x)$ is the empirical distribution, and $E_P(f_i)$ is the expectation of the characteristic function about the empirical distribution [27].

The MaxEnt model 3.4.1 was downloaded from (https://biodiversityinformatics.amnh.org/, accessed on 6 November 2021) in this study. MaxEnt uses environment variables as constraints to infer the response of species potential distribution to environmental factors. Therefore, current and future potential distribution ranges and habitat suitability

can be calculated [28,29]. In order to obtain more accurate prediction results, the experimental methods of Zhang et al. [30] were referred to and optimized. When constructing the model, the geographical location information data of the sample was divided into two parts, 75% was used to build model simulations, and the remaining 25% was used for model testing. Due to the limitations of sample information and to ensure more accurate convergence results, 100 repetitions were set with a maximum of 500 iterations, the convergence threshold was set to 1×10^{-6} for each training repetition, and the output was in Logistic format. In order to describe the distribution changes of *A. cordatum*, the simulated results were reclassified by the natural breakpoint method in ArcGIS 10.8 (Esri, Redlands, CA, USA), and divided into four levels, unsuitable area, marginally suitable area, moderately suitable area, and highly suitable area, respectively. Finally, maps of suitable habitats under history, current, and future climate scenarios were drawn in ArcGIS 10.8.

The MaxEnt output patterns could be explained using the area under the receiver operating characteristic curve (AUC), and each variable contribution could be evaluated by using the Jack-knife test. The AUC values represent the correlation between environmental variables and the geographical location of the subject [31] and are widely used for the evaluation of model prediction accuracy [32]. AUC values varied in the range between 0 and 1. The larger the AUC value, the closer the model simulation is to the real situation [33]. An AUC value lower than 0.6 was deemed to be a failure, which indicated that the model did not possess predictive capabilities. The simulation result was defined as a general result when the AUC value is between 0.7 and 0.8, a good result when the AUC value is between 0.8 and 0.9, and an excellent result when the AUC value is between 0.9 and 1, which indicated that the model was considered to possess high prediction accuracy [34].

The MaxEnt model includes a jack-knife method (regularized training gain, AUC, and test gain) and two estimations to analyze the contribution and importance of environment variables. The first estimation, the increase in regularized gain, is added to the contribution of the corresponding variable, or subtracted from it if the change to the absolute value of lambda is negative in each iteration of the training algorithm. In the second estimation, the values of each environment variable in training presence and background data are randomly permuted. The model is reevaluated on the permuted data, and the resulting drop in training AUC is shown in the table, normalized to percentages.

3. Results

3.1. Model Accuracy

In this study, 13 climatic variables were removed according to the Pearson correlation coefficients analysis (Figure 2) and Percent contribution (Table 1). Six climatic variables were ultimately selected and used to predict model (Table 2). These climatic variables include the Mean Diurnal Range (bio2), Mean Temperature of Coldest Quarter (bio11), Annual Precipitation (bio12), Precipitation of Driest Month (bio14), Precipitation of Seasonality (bio15), and Precipitation of Warmest Quarter (bio18).

Table 2. Contribution percentage of each environmental variable in the MaxEnt modeling.

Variable	Description	Contribution (%)	Permutation Importance
bio2	Mean Diurnal Range (°C)	8.1	0.9
bio11	Mean Temperature of Coldest Quarter (°C)	21	28.5
bio12	Annual Precipitation (mm)	10.4	8.5
bio14	Precipitation of Driest Month (mm)	32.5	13.6
bio15	Precipitation of Seasonality (mm)	12.7	20.3
bio18	Precipitation of Warmest Quarter (mm)	15.3	28.1

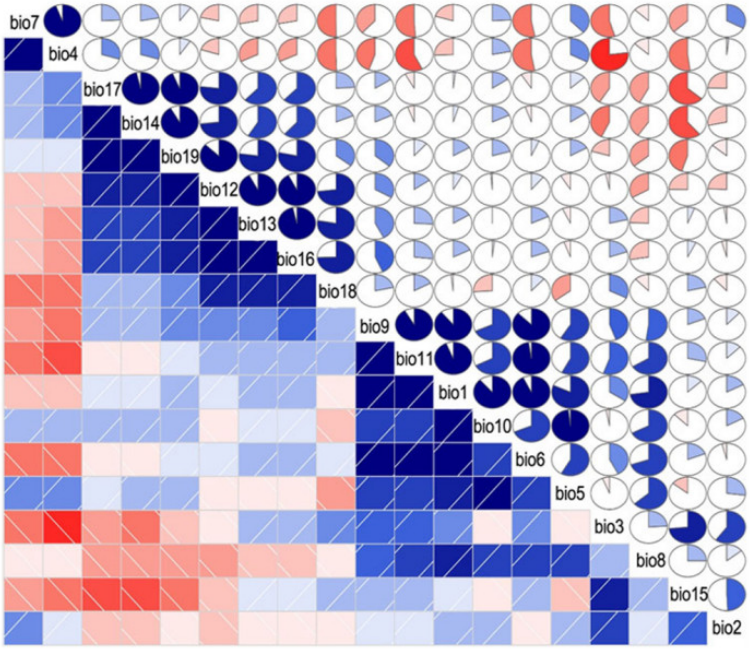

Figure 2. Correlations among 19 climatic variables. The blue color in the lower triangular cell and the slash from the lower left to the upper right indicate that the two variables in the cell are positively correlated. In turn, red and slashes from top left to bottom right indicate that the variables are negatively correlated. The darker the color and the higher the saturation, the greater the correlation between variables. Cells with a correlation close to 0 are largely colorless. The upper triangular cell presents the same information in a pie chart. The color functions as above, but the correlation size is represented by the size of the pie tile being filled. Positive correlations will fill the pie chart clockwise starting at 12 o'clock, while negative correlations will fill the pie chart counterclockwise.

Based on the 297 distribution information points and 6 climatic variables for *A. cordatum*, the MaxEnt model was simulated to predict the potential geographical distribution of *A. cordatum*. The mean AUC values were 0.973 and greater than 0.95 (Figure 3), indicating that the models performed well and generated reliable predictions for *A. cordatum*.

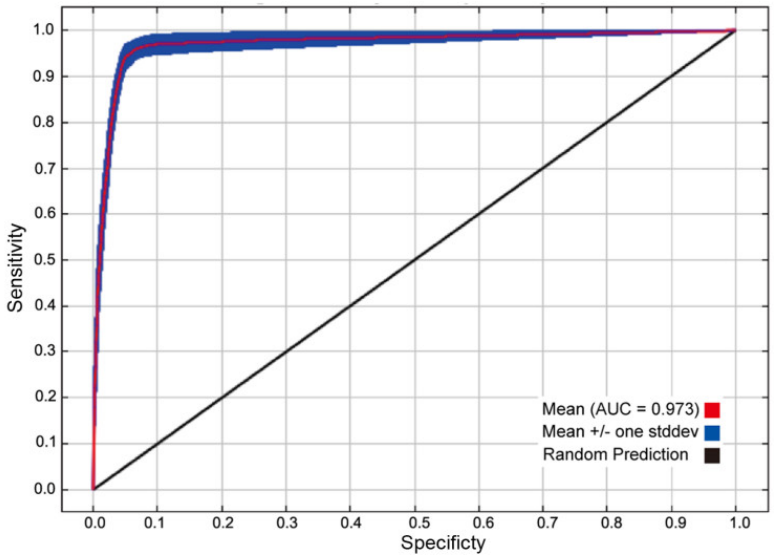

Figure 3. The area under the curve (AUC) values of *A. cordatum* obtained by receiver operating characteristic (ROC) analysis for testing the results of the MaxEnt model.

3.2. Importance of Variables and Climate Preference

The percentage contribution showed that six climatic variables for model construction were bio14 (Precipitation of Driest Month) > bio11 (Mean Temperature of Coldest Quarter) > bio18 (Precipitation of Warmest Quarter) > bio15 (Precipitation of Seasonality) > bio12 (Annual Precipitation) > bio2 (Mean Diurnal Range). Among them bio14, bio11, bio18, and bio15 are the top four climatic variables which contributed to 32.5%, 21%, 15.3%, and 12.7%, respectively (Table 2). The permutation importance indicated that the Mean Temperature of Coldest Quarter (bio11, 28.5), Precipitation of Warmest Quarter (bio18, 28.1), Precipitation of Seasonality (bio15, 20.3), and Precipitation of Driest Month (bio14, 13.6) were the top four climatic variables (Table 2). The regularized training gain, AUC, and test gain of climatic variables of the Jackknife test in MaxEnt, which indicated that six environmental variables, play an important role in the contribution of of *A. cordatum* (Figure 4). Each variable takes a similar proportion for different Jackknife test. According to the degree of contribution from highest to lowest, the order is Precipitation of Driest Month (bio14), Mean Temperature of Coldest Quarter (bio11), Precipitation of Seasonality (bio15), Precipitation of Warmest Quarter (bio18), Mean Diurnal Range (bio2), and Annual Precipitation (bio12).

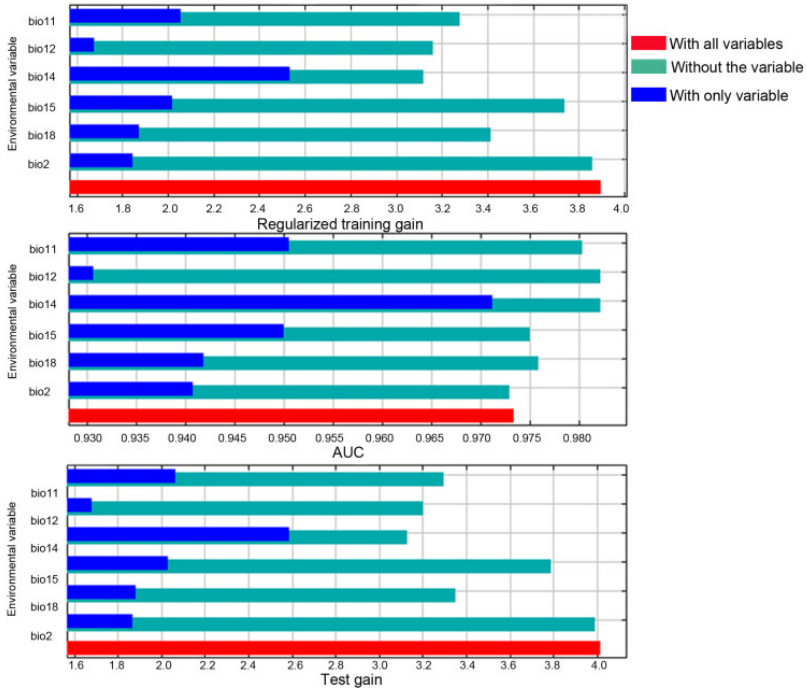

Figure 4. The importance of environmental variables of regularized training gain, AUC, and test gain using the Jackknife test. bio2, Mean Diurnal Range; bio11, Mean Temperature of Coldest Quarter; bio12, Annual Precipitation; bio14, Precipitation of Driest Month; bio15, Precipitation of Seasonality; bio18, Precipitation of Warmest Quarter.

3.3. Threshold Analysis of Important Environmental Variables

The probability response curves demonstrate how the logistic prediction for *A. cordatum* changes, while the remaining predicting factors are maintained at their average values (Figure 5). The threshold values of Mean Temperature of Coldest Quarter (bio11) for the probability of *A. cordatum* presence were found to be approximately −31 to 28 °C, the threshold values of Precipitation of Driest Month (bio14) were 0 to 211 mm, the threshold values of Precipitation of Seasonality (bio15) were 18 to 164 mm, and the threshold values of Precipitation of Warmest Quarter (bio18) were 10 to 4406 mm. The highest points of the response curves represent their optimal threshold, which means that the temperature/precipitation is most suitable for the growth of *A. cordatum*.

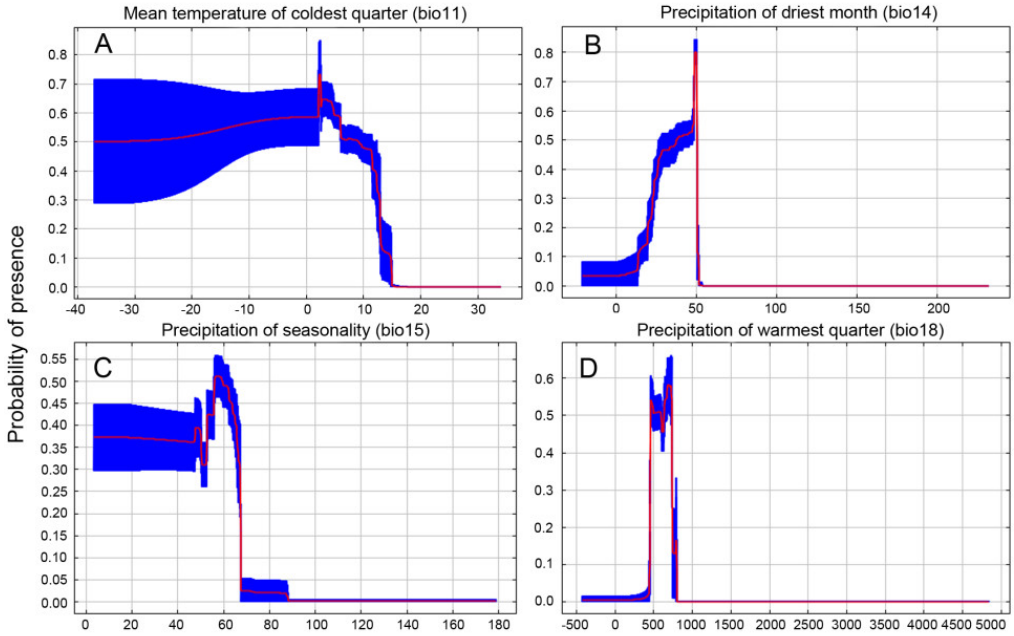

Figure 5. Probability response curves for the main predictor variables of the modeled distribution of *A. cordatum* based on the MaxEnt algorithm. (**A**) Mean Temperature of Coldest Quarter (bio11), (**B**) Precipitation of Driest Month (bio14), (**C**) Precipitation of Seasonality (bio15), and (**D**) Precipitation of Warmest Quarter (bio18). The red curves represent the mean response of the 100 replicate Maxent runs, and the blue shades represent mean +/− one standard deviation.

3.4. Potential Distribution Areas of A. cordatum in East Asia

The result of climatic change effects on the potential distribution of *A. cordatum* as analyzed by MaxEnt program is quite interesting (Figure 6, Table 3). Compared to the current distribution area, the potential distribution area in the historical (LIG: Last interglacial and LGM: Last glacial maximum) and future periods (2060s and the 2080s) demonstrated a process of expansion and then contraction. Particularly in the LIG period, the suitable distribution areas of *A. cordatum* almost disappeared, and only 0.29% (6×10^4 km^2) of the suitable area remained.

The current potentially suitable area of *A. cordatum* was predicted to be 9.4×10^5 km^2 (Table 3), which was primarily distributed in Chongqing, Guizhou, Hunan, Hubei, Anhui, Jiangsu, Jiangxi, Zhejiang, Guangxi, Guangdong, and Fujian provinces (Figure 6d). In addition, potential suitable areas were also detected in the southernmost areas of North and South Korea and Japan. The highly suitable areas, moderately suitable areas, and marginally suitable areas were 9×10^4 km^2, 3.6×10^5 km^2, and 4.9×10^5 km^2, respectively. Among them, the highly suitable areas were mainly distributed in Zhejiang, Fujian, Jiangxi, Guangxi, and Hunan provinces. In the LIG climatic scenario, the spatial location for suitable *A. cordatum* distribution areas was mainly concentrated in the area of northern Fujian, southern Zhejiang, and northern Jiangxi. Compared with the LIG, the total area of contemporary distribution increased by 8.8×10^5 km^2 (4.44%). The high, moderate, and marginal suitable area have been decreased 8×10^4 km^2, 3.5×10^5 km^2, and 4.5×10^5 km^2, respectively. In the LGM scenario, MIROC was used to simulate, due to the model obtained from climate change in East Asia having better compatibility with *A. cordatum* than CCSM. The spatial location for suitable *A. cordatum* was significantly expanded and moved westward in the LGM. The high, moderate, and marginal regions were 4×10^4 km^2, 4×10^4 km^2, and 1.2×10^5 km^2, respectively. The result of the algorithms showed that the suitable distribution areas of *A. cordatum* were mainly concentrated in the area of 25 °N in the central part of East Asia, and the highly suitable areas were concentrated in southern Chongqing, northern Hunan, northern Guizhou, and Zhejiang.

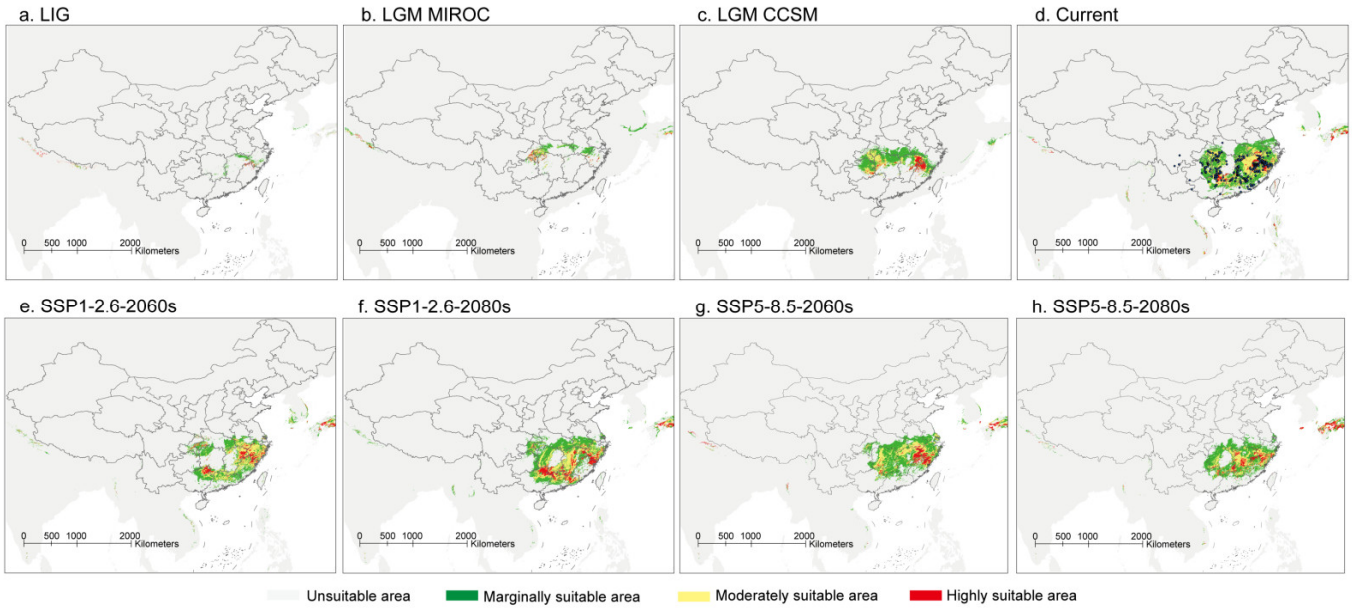

Figure 6. Prediction of potential distribution areas of *A. cordatum* in LIG (**a**), LGM MIROC (**b**), LGM CCSM (**c**), Current (**d**), SSP1-2.6-2060s (**e**), SSP1-2.6-2080s (**f**), SSP5-8.5-2060s (**g**), and SSP5-8.5-2080s (**h**) by MaxEnt. LIG: Last interglacial; LGM MIROC: Model for Interdisciplinary Research on Climate Earth System Model of the Last Glacial Maximum; LGM CCSM: Community Climate System Model of the Last Glacial Maximum.

Table 3. Characteristics of potential distribution areas and distribution percentages during different periods for *A. cordatum*.

Period		Marginally Suitable Area	Moderately Suitable Area	Highly Suitable Area	Total Suitable Area
Area of each suitable area (change in the area compared to current, 10^4 km^2)					
LIG		4 (−45)	1 (−35)	1 (−8)	6 (−88)
LGM (MIROC)		12 (−27)	4 (−32)	4 (−5)	20 (−74)
LGM (CCSM)		29 (−20)	11 (−25)	5 (−4)	45 (−49)
Current		49 (0.00)	36 (0.00)	9 (0.00)	94 (0.00)
SSP1-2.6	Future 2060s	34 (−15)	24 (−12)	8 (−1)	66 (−28)
	Future 2080s	45 (−4)	29 (−7)	13 (+4)	87 (−7)
SSP5-8.5	Future 2060s	43 (−6)	22 (−24)	8 (−1)	73 (−21)
	Future 2080s	38 (−11)	19 (−17)	9 (±0)	66 (−28)
Area of each suitable area (percentage change in the area compared to current, %)					
LIG		0.20% (−2.27%)	0.05% (−1.77%)	0.05% (−0.40%)	0.30% (−4.44%)
LGM (MIROC)		0.61% (−1.36%)	0.20% (−1.62%)	0.20% (−0.25%)	1.01% (−3.74%)
LGM (CCSM)		1.46% (−1.01%)	0.56% (−1.26%)	0.25% (−0.20%)	2.27% (−2.47%)
Current		2.47% (0.00%)	1.82% (0.00%)	0.45% (0.00%)	4.75% (0.00%)
SSP1-2.6	Future 2060s	1.72% (−0.76%)	1.21% (−0.61%)	0.40% (−0.05%)	3.33% (−1.41%)
	Future 2080s	2.27% (−0.20%)	1.46% (−0.35%)	0.66% (+0.20%)	4.39% (−0.35%)
SSP5-8.5	Future 2060s	2.17% (−0.30%)	1.11% (−1.21%)	0.40% (−0.05%)	3.69% (−1.06%)
	Future 2080s	1.92% (−0.56%)	0.96% (−0.86%)	0.45% (±0.00%)	3.33% (−1.41%)

In the future, the suitable habitat of *A. cordatum* will have different development trends under the SSP1-2.6 and SSP5-8.5, but compared with the current, the potential suitable area of *A. cordatum* is contracted by varying degrees (Figure 6e–h).

Under the SSP1-2.6-2060s climatic scenario, MaxEnt predicted that the main spatial location for the suitable distribution areas of *A. cordatum* are Chongqing, Hunan, Hubei, Jiangxi, Guangxi, Guangdong, Fujian, Zhejiang, and Anhui provinces. Compared with the current areas, the suitable distribution areas were significantly reduced in Guizhou,

Chongqing, and Hunan, and the potential distribution almost disappeared in Jiangxi and Jiangsu. Under the SSP1-2.6-2080s climatic scenario, the suitable distribution areas seem to be a slight increase compared to 2060s. In the three suitable habitats, the highly suitable area would expand by 4×10^4 km^2, and the marginally and moderately suitable areas had a trend of contraction.

Under the SSP5-8.5 climate scenario, the suitable distribution areas of *A. cordatum* will have a tendency to move to northwards in the 2060s and 2080s, and the distribution areas will continue to decrease. Under the SSP5-8.5-2060s climatic scenario, the total suitable area would decrease by 2.1×10^5 km^2 (1.06%) with the reduction of the three suitable habitats (marginally suitable area, moderately suitable area, and highly suitable area). The highly suitable area will mainly concentrate in Zhejiang, Fujian, and Jiangxi. In SSP5-8.5-2080s climatic scenario, compared with the current, the total potential distribution area would reduce by 2.8×10^5 km^2. The distribution area will likely be reduced in Guizhou, Guangdong, Guangxi, and Zhejiang, and the habitat will have almost disappeared in Chongqing. The highly suitable area of *A. cordatum* has fragmented distribution in many provinces, including Zhejiang, Fujian, Jiangxi, Hunan, and Guangxi. In general, in the future, the total suitable habitat of *A. cordatum* was predicted to decrease, and it exhibited a trend of moving northeastward.

The distribution areas changes of *A. cordatum* can be found more intuitively by overlapping analysis of the potential distribution ranges in the different climatic scenario of future (Figure 7). It can be seen that due to the climate change in the future, the potential distribution areas of *A. cordatum* will contract. The main spatial location ranges of *A. cordatum* has not moved significantly on the whole, but the suitable regions of *A. cordatum* would be significantly lost in the future (yellow area) compared with the current. The shrinking area (yellow area) was larger significantly in the future than the expanding area (green/blue area), and the distribution area of suitable *A. cordatum* almost disappeared in Guizhou and Fujian. The southernmost boundary in the distribution area of *A. cordatum* moved northward under the SSP5-8.5 climate scenario (Current 2080s).

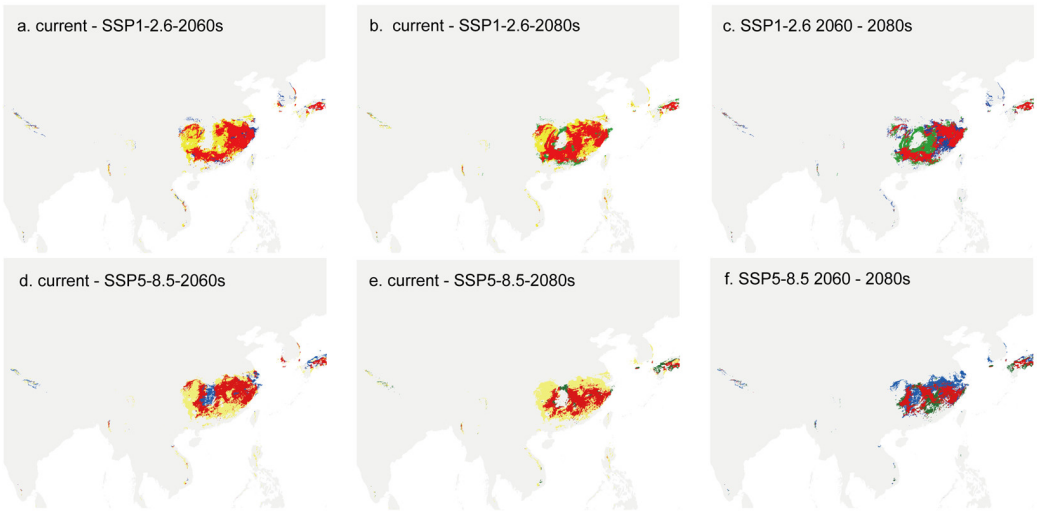

Figure 7. Distribution area changes of *A. cordatum* in the future under SSP1-2.6 and SSP5-8.5 climatic scenarios. (**a**–**c**) The distribution areas of *A. cordatum* in current to 2060s, current to 2080s, and 2060s to 2080s under SSP1-2.6 climatic scenarios. (**d**–**f**) The distribution areas of *A. cordatum* in current to 2060s, current to 2080s, and 2060s to 2080s under SSP5-8.5 climatic scenarios. The red area represents the distribution area overlapped or unchanged between the two different periods. The yellow area represents the potential distribution area of current. The blue and green areas represent the potential range of expansion of 2060 and 2080 years, respectively.

4. Discussion

The impact of climatic changes has a significant effect on plant survival and distribution [35], which has led to this becoming a direction worthy of attention of botany and ecology [36–38]. To study the impact climate changes have on *A. cordatum*, MaxEnt provided a method for judging the influence of various environmental variables on species distribution based on the geographical distribution of species in a known environmental background [28]. This enabled an analysis of the influence of the current climate on the distribution of *A. cordatum* based on the existing spatial location for the suitable distribution areas of *A. cordatum* and a simulation of the climate environment in the future and the past to be performed. The results obtained by MaxEnt were found to be reliable when environmental variables are complex and species have a large distribution area [11]. Previous studies have successfully predicted the history (LIM and LGM periods) and future potential distribution areas of some species, e.g., *Acer davidii* Franch [39], *Platycladus orientalis* (L.) Franco [40]. In this study, the impact climate changes have on the suitable distribution area of *A. cordatum* was analyzed using MaxEnt and the results were used for predicting suitable distribution areas in five different scenarios (LIM, LGM, current, 2060s, and 2080s). The high AUC values and the result of jackknife tests both showed our prediction to have high accuracy. It can also be seen that MaxEnt maintains high accuracy when dealing with limited geographical distribution information [41,42]. Although MaxEnt has been common in predicting the potential distribution of species in suitable habitats [39,40], it still has some limitations. Based on the occurrence-environment relationship that is established by MaxEnt, the result produces over-fitting, a phenomenon that will affect the prediction results [27,43]. The distribution area predicted by MaxEnt is small and polydispersed, resulting in marginalized suitable areas being ignored. For example, Zhang et al. [30] simulated the distribution of *Euspathis japonica* (Thunb.) Kanitz and found that the marginal suitable areas in Jiangsu and Anhui were not detected. However, through continuous optimization of the MaxEnt model in recent years [28], the accuracy of simulation results has been improved to a certain extent.

In this study, we found that the most important ones for explaining the environmental requirements of *A. cordatum* were three derived from precipitation and one derived from temperature, including Mean Temperature of Coldest Quarter (bio11), Precipitation of Driest Month (bio14), Precipitation of Seasonality (bio15), and Precipitation of Warmest Quarter (bio18). This demonstrates that precipitation was critical for the survival of *A. cordatum*. As with previous studies, our simulations also supported that the northern border of evergreen broadleaf forest in coastal China was more southward than that in Japan due to precipitation [44]. At the same time, temperature and moisture stability in the environment affects the growth of *A. cordatum*. The changes in these environmental indicators led to the changes in the suitable *A. cordatum* distribution area. The potential distribution areas of *A. cordatum* have significant changes in history (LIG, LGM to current), which may be related to the large fluctuation of global climate since the late Pleistocene, especially the last glacial–interglacial cycle [45,46]. It was also found that during the last glacial period, the number of suitable areas for *A. cordatum* increased compared to the current period, but the land area percentage decreased. This is because during the warming period following the last glacial period, global temperatures increased, resulting in a rising sea level and the disappearance of the land bridge between Japan and the Korean peninsula [47], where some of the suitable *A. cordatum* distribution areas were located. Meanwhile, some suitable areas may disappear and the emergence of new land will provide newly suitable areas for certain plants due to changes in sea level [48].

Meanwhile, we have also found that the potential distribution areas of *A. cordatum* had a tendency of moving to the northeastward under future climate scenarios (Figure 6). Although the direction of movement was slightly different at different periods, it would move to northward or northeastward in the future, relative to the current climatic period. We have also found that the prediction results slightly varied when analyzing the different emission scenarios (SSP1-2.6 and SSP5-8.5) under the same periods. Under the SSP1-2.6,

the highly suitable distribution areas of *A. cordatum* were mainly concentrated in Jiangxi, Zhejiang, Fujian, Guangdong, and Guangxi. Under the SSP5-8.5, the highly suitable distribution areas of *A. cordatum* were mainly concentrated in Jiangxi, Zhejiang, and Fujian. The difference in the development trend of two SSP scenarios may be due to different development pathways in the future society. Research showed that habitats of *A. cordatum* will significantly reduce in many provinces in the future, including Guizhou, Fujian, and Anhui. Under the SSP5-8.5 climatic scenario, the distribution of Chongqing almost disappeared. In the future, the main distribution areas of *A. cordatum* were still around 25 °N. Global temperature increasing is an inevitable trend [49]. The rising temperature may expedite physiological processes and thus affect the growth of plants. The distribution areas changes of *A. cordatum* indicated that this species is sensitive to high temperatures and has the potential to grow at high temperatures and in humid areas. The distribution areas of *A. davidii* have similar future mobility trends [39]. Previous studies have mostly assumed that plants have a tendency to migrate to higher latitudes in an environment with an increased temperature [50], but the distribution of *A. cordatum* remained in lower latitudes in the future. These results may be related to various environmental factors except climatic variables, such slope and solar radiation. *A. cordatum* mainly grows in valleys and streams and has complex topographic environments. The altitude and slope in different terrain environments will have an impact on plant growth. For example, the difference in light between the south slope and the north slope may lead to divergence of temperature and soil humidity, which may indirectly affect the plant geographic distribution and growth. Solar radiation is one of the important environmental parameters driving photosynthesis, transpiration [51], and the formation and development of plant organs [52]. Previous studies have shown that global solar radiation has been decreasing in China [53,54], which is unfavorable to the growth and development of most plants.

The climate variables is indeed an ecological factor that has an important effect on the distribution of plants, but it has been confirmed that other ecological variables also impact on the distribution species, e.g., soil composition [55], orography [56], biotic interactions [7], and so on. For example, bacteria in the soil affect the growth of chrysanthemums [57], and endosymbionts enhance the resistance to stress of pants. Topographically complex terrain can create diverse climates and strongly affect the variations in plant trait [58]. Lamb et al. [59] conducted experiments with nine grassland plants and found that the above-ground and root competition of plants significantly impacts plant communities and diversity. In general, climatic factors not only directly affect the plant growth, but also affect soil properties, such as soil PH and particle size, which could indirectly affect plant growth. In addition, the impact human activities and the alien invasion species are also factors that must not be ignored. However, due to limited information and methods, the effects of these factors were not studied in this study. Therefore, it is hoped that subsequent research will compensate for this defect and establish a complete distribution system of *A. cordatum*. Despite this, our study can still provide theoretical support for further introduction and cultivation for *A. cordatum*.

5. Conclusions

In conclusion, using the MaxEnt model, four environmental variables that have a significant important effect on the survival and distribution of *A. cordatum* were identified, including Mean Temperature of Coldest Quarter (bio11), Precipitation of Warmest Quarter (bio18), Precipitation of Driest Month (bio14), and Precipitation of Seasonality (bio15). In addition, the potential paleo-climatic (LGM and LIG) roots of the distribution patterns of *A. cordatum* were revealed, and future (the 2060s and 2080s) suitable distribution area changes were predicted. The study results suggested that suitable distribution areas of *A. cordatum* will decrease in the future. Compared to the current period, under SSP1-2.6 and SSP5-8.5 climatic scenario, MaxEnt predicts that suitable distribution areas will decrease 1.41% (2060s) and 0.35% (2080s), 1.06% (2060s), and 1.41% (2080s), respectively. Generally, based on the predictions of this research, the future environment will have a certain impact

for the survival of *A. cordatum*, and its suitable distribution will have a tendency to move northeast of China. It is expected that this research will provide a theoretical reference for *A. cordatum* conservation plans and the establishment of protected areas.

Author Contributions: Conceptualization, M.-L.L., H.-Y.S. and Z.-H.L.; Data curation, M.-L.L., X.J. and T.Z.; Formal analysis, H.-Y.S., T.Z. and Z.-D.S.; Funding acquisition, Y.-N.Z. and Z.-H.L.; Investigation, H.-Y.S., X.J. and Q.-J.Z.; Methodology, Z.-H.L.; Resources, M.-L.L., H.-Y.S. and Z.-H.L.; Software, M.-L.L. and H.-Y.S.; Supervision, J.-N.L.; Validation, M.-L.L., H.-Y.S. and Z.-D.S.; Visualization, H.-Y.S.; Writing—original draft, H.-Y.S.; Writing—review & editing, M.-L.L., J.-N.L. and Z.-H.L. All authors have read and agreed to the published version of the manuscript.

Funding: This research was funded by the National Natural Science Foundation of China (31970359), the Key Program of Research and Development of Shaanxi Province (2022ZDLSF06-02), the Shaanxi Science and Technology Innovation Team (2019TD-012), the Research Project of Teaching Reform of Northwest University (363062102018) and the Fourth National Survey of Traditional Chinese Medicine Resources (2019-39).

Conflicts of Interest: The authors declare no conflict of interest.

References

1. Li, X.; Chen, J.; Guo, W. A review of the influence factors of plant phenology under different climate types. *J. Earth Environ.* **2018**, *9*, 16–27.
2. Thomas, C.D.; Cameron, A.; Green, R.E.; Bakkenes, M.; Beaumont, L.J.; Collingham, Y.C.; Erasmus, B.F.N.; de Siqueira, M.F.; Grainger, A.; Hannah, L.; et al. Extinction risk from climate change. *Nature* **2004**, *427*, 145–148. [CrossRef] [PubMed]
3. Smale, D.A.; Wernberg, T. Extreme climatic event drives range contraction of a habitat-forming species. *Proc. R. Lond. Ser. B Biol. Sci.* **2013**, *280*, 20122829. [CrossRef] [PubMed]
4. Pulliam, H.R. On the relationship between niche and distribution. *Ecol. Lett.* **2000**, *3*, 349–361. [CrossRef]
5. Hutchinson, G.E. Concluding remarks—Cold spring harbor symposia on quantitative biology. Reprinted in 1991: Classics in theoretical biology. *Bull. Math. Biol.* **1957**, *53*, 193–213. [CrossRef]
6. Chen, X.D.; Yang, J.; Feng, L.; Zhou, T.; Zhang, H.; Li, H.M.; Bai, G.Q.; Meng, X.; Li, Z.H.; Zhao, G.F. Phylogeography and population dynamics of an endemic oak (*Quercus fabri* Hance) in subtropical China revealed by molecular data and ecological niche modeling. *Tree Genet. Genomes* **2020**, *16*, 2. [CrossRef]
7. Guisan, A.; Zimmermann, N.E. Predictive habitat distribution models in ecology. *Ecol. Model.* **2000**, *135*, 147–186. [CrossRef]
8. Peterson, A.T.; Papes, M.; Eaton, M. Transferability and model evaluation in ecological niche modeling: A comparison of GARP and Maxent. *Ecography* **2007**, *30*, 550–560. [CrossRef]
9. Pecchi, M.; Marchi, M.; Burton, V.; Giannetti, F.; Moriondo, M.; Bernetti, I.; Bindi, M.; Chirici, G. Species distribution modelling to support forest management. A literature review. *Ecol. Model.* **2019**, *411*, 108817. [CrossRef]
10. Li, X.H.; Wang, Y. Applying various algorithms for species distribution modelling. *Integr. Zool.* **2013**, *8*, 124–135. [CrossRef]
11. Farashi, A.; Kaboli, M.; Karami, M. Predicting range expansion of invasive raccoons in northern Iran using ENFA model at two different scales. *Ecol. Inform.* **2013**, *15*, 96–102. [CrossRef]
12. Ahmed, S.E.; Mcinerny, G.; O'Hara, K.; Harper, R.; Salido, L.; Emmott, S.; Joppa, L.N. Scientists and software—Surveying the species distribution modelling community. *Divers. Distrib.* **2015**, *21*, 258–267. [CrossRef]
13. FitzGerald, A.M. Division within the North American boreal forest: Ecological niche divergence between the Bicknell's Thrush (*Catharus bicknelli*) and Gray-cheeked Thrush (*C. minimus*). *Ecol. Evol.* **2017**, *7*, 5285–5295. [CrossRef]
14. Peng, H.H.; Guan, B.F.; Chen, H.L.; Peng, H.; Peng, Y.F.; Yu, Y.F.; You, Y.J. Study on seed characteristics and sowing techniques of four species of maple. *Acta Agric. Jiangxi* **2014**, *26*, 19–22.
15. Chen, H.L.; Peng, H.H.; Zhu, Q.D.; Guan, B.F.; Peng, H.; Xu, J.H.; Peng, Y.F. Study on the grafting technique of three kinds of maple. *Jiangxi Sci.* **2014**, *32*, 35–38.
16. Gao, P. Effects of Matrix and Illumination Intensity on Seedling of *Acer cordatum* "Huoyan". Master's Thesis, Jiangxi Agricultural University, Nanchang, China, 2018.
17. Liu, K.W.; Yang, H.; Yang, J.; Tong, H.Y. Phenology and Adaptability of Three Evergreen Maples in Nanjing. *Shaanxi J. Agric. Sci.* **2021**, *67*, 30–32.
18. Qiu, Y.X.; Cheng, S.X.; Du, T.Z.; Wang, F.; Yang, J.J. Seasonal Changes of Leaf Protease Activity in Several Varieties of Maple Family. *Acta Agric. Univ. Jiangxiensis* **2003**, *25*, 652–655.
19. Boitani, L.; Maiorano, L.; Baisero, D.; Falcucci, A.; Visconti, P.; Rondinini, C. What spatial data do we need to develop global mammal conservation strategies? *Philos. Trans. R. Soc. London. Ser. B Biol. Sci.* **2011**, *366*, 2623–2632. [CrossRef]
20. Fick, S.E.; Hijmans, R.J. WorldClim 2: New 1-km spatial resolution climate surfaces for global land areas. *Int. J. Climatol.* **2017**, *37*, 4302–4315. [CrossRef]
21. Baldwin, R.A. Use of Maximum Entropy Modeling in Wildlife Research. *Entropy* **2009**, *11*, 854. [CrossRef]

22. Dormann, C.F.; Elith, J.; Bacher, S.; Buchmann, C.; Carl, G.; Carre, G.; Marquez, J.R.G.; Gruber, B.; Lafourcade, B.; Leitao, P.J.; et al. Collinearity: A review of methods to deal with it and a simulation study evaluating their performance. *Ecography* **2013**, *36*, 27–46. [CrossRef]
23. Nozawa, T.; Nagashima, T.; Ogura, T.; Yokohata, T.; Okada, N.; Shiogama, H. *Climate Change Simulations with a Coupled Ocean-Atmosphere GCM Called the Model for Interdisciplinary Research on Climate: MIROC*; Center for Global Environmental Research, National Institute for Environmental Studies: Tsukuba, Japan, 2007.
24. Hijmans, R.J.; Cameron, S.E.; Parra, J.L.; Jones, P.G.; Jarvis, A. Very high resolution interpolated climate surfaces for global land areas. *Int. J. Climatol.* **2005**, *25*, 1965–1978. [CrossRef]
25. Rosenkrantz, R.D. *E. T. Jaynes: Papers on Probability, Statistics and Statistical Physics*; Springer: Dordrecht, The Netherlands, 1989.
26. Renner, I.W.; Warton, D.I. Equivalence of MAXENT and Poisson Point Process Models for Species Distribution Modeling in Ecology. *Biometrics* **2013**, *69*, 274–281. [CrossRef] [PubMed]
27. Merow, C.; Smith, M.J.; Silander, J.A. A practical guide to MaxEnt for modeling species' distributions: What it does, and why inputs and settings matter. *Ecography* **2013**, *36*, 1058–1069. [CrossRef]
28. Phillips, S.J.; Anderson, R.P.; Schapire, R.E. Maximum entropy modeling of species geographic distributions. *Ecol. Model.* **2006**, *190*, 231–259. [CrossRef]
29. Phillips, S.J.; Dudík, M. Modeling of species distributions with Maxent: New extensions and a comprehensive evaluation. *Ecography* **2008**, *31*, 161–175. [CrossRef]
30. Zhang, K.L.; Sun, L.P.; Tao, J. Impact of Climate Change on the Distribution of *Euscaphis japonica* (Staphyleaceae) Trees. *Forests* **2020**, *11*, 525. [CrossRef]
31. van Erkel, A.R.; Pattynama, P.M. Receiver operating characteristic (ROC) analysis: Basic principles and applications in radiology. *Eur. J. Radiol.* **1998**, *27*, 88–94. [CrossRef]
32. Reineking, B.; Schroder, B. Constrain to perform: Regularization of habitat models. *Ecol. Model.* **2006**, *193*, 675–690. [CrossRef]
33. Hanley, J.A.; McNeil, B.J. The meaning and use of the area under a receiver operating characteristic (ROC) curve. *Radiology* **1982**, *143*, 29–36. [CrossRef]
34. Swets, J.A. Measuring the accuracy of diagnostic systems. *Science* **1988**, *240*, 1285–1293. [CrossRef]
35. Manthey, M.; Box, E.O. Realized climatic niches of deciduous trees: Comparing western Eurasia and eastern North America. *J. Biogeogr.* **2007**, *34*, 1028–1040. [CrossRef]
36. Espeland, E.K.; Kettenring, K.M. Strategic plant choices can alleviate climate change impacts: A review. *J. Environ. Manag.* **2018**, *222*, 316–324. [CrossRef]
37. Harbert, R.S.; Nixon, K.C. Climate reconstruction analysis using coexistence likelihood estimation (CRACLE): A method for the estimation of climate using vegetation. *Am. J. Bot.* **2015**, *102*, 1277–1289. [CrossRef]
38. Lv, J.-j.; Wu, J.-g. Advances in the Effects of Climate Change on the Distribution of Plant Species and Vegetation in China. *Environ. Sci. Technol.* **2009**, *32*, 85–95.
39. Su, Z.D.; Huang, X.J.; Zhong, Q.Y.; Liu, M.L.; Song, X.Y.; Liu, J.N.; Fu, A.G.; Tan, J.L.; Kou, Y.X.; Li, Z.H. Change of Potential Distribution Area of a Forest Tree *Acer davidii* in East Asia under the Context of Climate Oscillations. *Forests* **2021**, *12*, 689. [CrossRef]
40. Li, G.Q.; Du, S.; Wen, Z.M. Mapping the climatic suitable habitat of oriental arborvitae (*Platycladus orientalis*) for introduction and cultivation at a global scale. *Sci. Rep.* **2016**, *6*, 30009. [CrossRef]
41. Elith, J.; Graham, C.H.; Anderson, R.P.; Dudik, M.; Ferrier, S.; Guisan, A.; Hijmans, R.J.; Huettmann, F.; Leathwick, J.R.; Lehmann, A.; et al. Novel methods improve prediction of species' distributions from occurrence data. *Ecography* **2006**, *29*, 129–151. [CrossRef]
42. Hernandez, P.A.; Graham, C.H.; Master, L.L.; Albert, D.L. The effect of sample size and species characteristics on performance of different species distribution modeling methods. *Ecography* **2006**, *29*, 773–785. [CrossRef]
43. Royle, J.A.; Chandler, R.B.; Yackulic, C.; Nichols, J.D. Likelihood analysis of species occurrence probability from presence-only data for modelling species distributions. *Methods Ecol. Evol.* **2012**, *3*, 545–554. [CrossRef]
44. Fang, J.Y. Arrangement of east-Asian vegetation-climate types on coordinates of temperature and precipitation. *Acta Ecol. Sin.* **1994**, *14*, 290–294.
45. Hewitt, G. The genetic legacy of the Quaternary ice ages. *Nature* **2000**, *405*, 907–913. [CrossRef]
46. Stewart, J.R.; Lister, A.M.; Barnes, I.; Dalen, L. Refugia revisited: Individualistic responses of species in space and time. *Proc. R. Soc. B Biol. Sci.* **2010**, *277*, 661–671. [CrossRef]
47. Zhou, S.; Zhao, J.; Wang, J.; Xu, L.; Cui, J.; Ou, X.; Xie, J. Quaternary CryosphereStudy on Global Change in Long Terms. *Bull. Chin. Acad. Sci.* **2020**, *35*, 475–483.
48. Chust, G.; Borja, Á.; Caballero, A.; Irigoien, X.; Sáenz, J.; Moncho, R.; Marcos, M.; Liria, P.; Hidalgo, J.; Valle, M.; et al. Climate change impacts on coastal and pelagic environments in the southeastern Bay of Biscay. *Clim. Res.* **2011**, *48*, 307–332. [CrossRef]
49. Araújo, M.B.; New, M. Ensemble forecasting of species distributions. *Trends Ecol. Evol.* **2007**, *22*, 42–47. [CrossRef]
50. Li, S.; Lu, J.; Yan, J.; Liu, X.; Kong, F.; Wang, J. Spatiotemporal variability of temperature in northern and southern Qinling Mountains and its influence on climatic boundary. *Acta Geogr. Sin.* **2018**, *73*, 13–24.
51. Aber, J.D.; Freuder, R. Variation among solar radiation data sets for the Eastern US and its effects on predictions of forest production and water yield. *Clim. Res.* **2000**, *15*, 33–43. [CrossRef]

52. Ding, L.; Wang, K.J.; Jiang, G.M.; Liu, M.Z.; Gao, L.M. Post-anthesis changes in photosynthetic traits of maize hybrids released in different years. *Field Crops Res.* **2005**, *93*, 108–115. [CrossRef]
53. Cui, H.Y.; Camberato, J.J.; Jin, L.B.; Zhang, J.W. Effects of shading on spike differentiation and grain yield formation of summer maize in the field. *Int. J. Biometeorol.* **2015**, *59*, 1189–1200. [CrossRef]
54. Ren, B.Z.; Cui, H.Y.; Camberato, J.J.; Dong, S.T.; Liu, P.; Zhao, B.; Zhang, J.W. Effects of shading on the photosynthetic characteristics and mesophyll cell ultrastructure of summer maize. *Sci. Nat.* **2016**, *103*, 67. [CrossRef] [PubMed]
55. Real, R.; Márquez, A.L.; Estrada, A.; Muoz, A.R.; Vargas, J.M. Modelling chorotypes of invasive vertebrates in mainland Spain. *Divers. Distrib.* **2010**, *14*, 364–373. [CrossRef]
56. Márquez, A.L.; Real, R.; Olivero, J.; Estrada, A. Combining climate with other influential factors for modelling the impact of climate change on species distribution. *Clim. Chang.* **2011**, *108*, 135–157. [CrossRef]
57. Ma, H.K.; Pineda, A.; van der Wurff, A.W.G.; Bezemer, T.M. Carry-over effects of soil inoculation on plant growth and health under sequential exposure to soil-borne diseases. *Plant Soil* **2018**, *433*, 257–270. [CrossRef]
58. Opedal, Ø.H.; Armbruster, W.S.; Graae, B.J. Linking small-scale topography with microclimate, plant species diversity and intra-specific trait variation in an alpine landscape. *Plant Ecol. Divers.* **2015**, *8*, 305–315. [CrossRef]
59. Lamb, E.G.; Kembel, S.W.; Cahill, J.F., Jr. Shoot, but not root, competition reduces community diversity in experimental mesocosms. *J. Ecol.* **2009**, *97*, 155–163. [CrossRef]